IOP Conf. Series: Materials Science and Engineering **739** (2020) 012014 doi:10.1088/1757-899X/739/1/012014

Effect of Road Surface Contour to the Fatigue Life of a Coil Spring Based on Strain-Life Approach

T E Putra[1], Husaini[1], M Ikbal[1]

[1]Department of Mechanical Engineering, Syiah Kuala University, Darussalam 23111, Banda Aceh, Indonesia

edi@unsyiah.ac.id

Abstract. This study aims to determine the effect of road surface contours to the fatigue life of an automotive coil spring. A strain gauge was affixed at the critical point based on the stress distributions. The vehicle passed smooth and rough roads with the speeds above 30 km/h and less than 20 km/h, respectively. The strain signals obtained were analyzed using the Coffin-Manson, Morrow, and Smith-Watson-Topper models. According to the analysis, when the vehicle passed the rough road, the coil spring received a higher stress leading to a shorter fatigue life, of 1,284 cycles to failure. This value was 526 % lower compared to the smooth road because it consisted of bumps and holes.

1. Introduction

Fatigue failure of a vehicle is affected by the physical condition of road surfaces. This is because its stability is reliant on the road surface and tire grinding [1]. Dynamic friction generates vibrations, which increases just as a vehicle moves on a rough road surface at high speeds. Repeated vibration damages vehicle components.

The coil spring is one of the major components of a vehicle which aims at reducing vibrations [2, 3]. However, it often fails owing to the repeated existence of residual stresses [4-6]. The coil spring is expected to not only be able to withstand vibrations, but also loads due to vehicle maneuvers, such as speed, braking or bending while in motion [2, 3]. It must also be able to reduce, withstand, and absorb impact twisting, and fatigue loads. Therefore, the aim of this study is to predict the fatigue life of a coil spring when a vehicle accelerates on smooth and rough road surfaces.

2. Materials and method

Chemical composition test is used to analyze and determine the compositions inherent in a material. Its size must be 1 - 10 cm (figure 1), to enable easy grinding and free from contaminants which agitates the testing results. The sample was inserted into PDA 7000 YS and was injected with an argon fluidized electrode for about 1 minute.

Content from this work may be used under the terms of the Creative Commons Attribution 3.0 licence. Any further distribution of this work must maintain attribution to the author(s) and the title of the work, journal citation and DOI.
Published under licence by IOP Publishing Ltd

Figure 1. A chemical composition testing sample.

The finite element analysis (FEA) works by dividing the component into small elements. Modeling is very important in FEA therefore a computer aided design is used to produce a model that is in accordance with the original. The efficiency of the FEA is dependent on the pre-processing stage, where the boundary conditions and the load are inserted. In the current study, tetrahedron was used for the meshing [7] and produced 10,999 nodes and 3,710 elements. Considering the vehicle and passenger's weight was 1,045 kg and 420 kg, respectively, with the total weight divided into four by assuming the load was evenly distributed to all wheels, in such a way that the load was 366.25 kg or 3,591.7 N. The load was administered at the bottom of the coil spring while the upper section was fixed support.

von Mises stress [8] is analyzed and acquired from hoop, longitudinal, and radial directions known as the three-dimensional main stress relationship. The yield citerion develops when the equivalent stress σ_e is equal to the yield stress σ_{ys}, which can be defined by:

$$\sigma_e = \frac{1}{\sqrt{2}}\left[\left(\sigma_x - \sigma_y\right)^2 + \left(\sigma_y - \sigma_z\right)^2 + \left(\sigma_z - \sigma_x\right)^2 + 6\left(\tau_{xy}^2 + \tau_{yz}^2 + \tau_{zx}^2\right)\right]^{1/2} \quad (1)$$

where σ_x, σ_y, σ_z are the normal stresses in the direction of the x, y and z-axes, while τ_{xy}, τ_{yz}, τ_{zx} are the shear stresses.

The strain signal measurement was carried out by attaching a 3-mm strain gauge with a resistance of 350 Ω at the coil spring. Furthermore, it was installed at a higher stress distribution area therefore the strain gauge easily detected the signals. The strain signal measurement must have a sampling frequency greater than 400 Hz [9]. Therefore, the frequency of 500 Hz used, was adequate to discover and store all destructive load cycles on the coil spring. After installing the equipment, the vehicle was driven on the smooth and rough road surfaces with its speed above 30 km/h and less than 20 km/h. Figure 2 shows the strain gauge installation.

Figure 2. Installation of strain gauge.

Fatigue signals are generally characterized by statistical parameters which are used to monitor patterns and classify random signals. Parameters often used to observe strain signals include mean, standard deviation (SD), root-mean square (r.m.s.), and kurtosis.

For signals F_j with a spesific number of data n, the mean value $\bar{x}$ is calculated by:

$$\bar{x} = \frac{1}{n}\sum_{j=1}^{n} Fj \tag{2}$$

SD determines how data are distributed in a sample. It is also attributed to the number of average variability in a data set. It value for numbers F_j above thirty can be stated by:

$$SD = \sqrt{\frac{1}{n}\sum_{j=1}^{n}(F_j - \bar{x})^2} \tag{3}$$

r.m.s. helps to estimate the total amount of energy in a discrete data F_j. This is expressed by:

$$r.m.s = \sqrt{\frac{1}{n}\sum_{j=1}^{n} F_j^2} \tag{4}$$

Kurtosis is a statistical parameter sensitive to spikes. The equation used to estimate kurtosis K in a discrete data F_j is:

$$K = \frac{1}{n(SD)^4}\sum_{j=1}^{n}(F_j - \bar{x})^4 \tag{5}$$

The strain-life technique accuratelly predicts fatigue life. This takes into account plastic events that occur in certain areas. It is quite good to use, does not require high costs or exhaustive crack observation provided failure occurs, and it is applied to small components. Elastic and plastic strain is combined to produce a relationship between the strain and the fatigue life, called the Coffin-Manson model [10,11] and this can be expressed by:

$$\varepsilon = \frac{\sigma'_f}{E}\left(2N_f\right)^b + \varepsilon'_f\left(2N_f\right)^c \tag{6}$$

where ε is the strain amplitude, σ'_f is the fatigue strength coefficient, E is the material modulus of elasticity, N_f is the number of cycles to failure for a particular stress range and mean, b is the fatigue strength exponent, ε'_f is the fatigue ductility coefficient and c is the fatigue ductility exponent.

Mean stress is an important factor in the analysis of fatigue and this affects its low and high cycles. Its effect can be investigated using the Morrow model [12], expressed by:

$$\varepsilon = \frac{\sigma'_f - \sigma_{\text{mean}}}{E}(2N_f)^b + \varepsilon'_f(2N_f)^c \tag{7}$$

where σ_{mean} is the normal mean stress. Furthermore, K.N. Smith, P. Watson, and T.H. Topper recomended the SWT parameter [13], a mean stress correction model mathematically defined as:

$$\sigma_{\max}\varepsilon = \frac{\sigma'^2_f}{E}(2N_f)^{2b} + \sigma'_f\varepsilon'_f(2N_f)^{b+c} \tag{8}$$

where $\sigma_{\max}$ is the maximum stress.

Fatigue damage is determined by the addition of normal and shear energy of the peak-valley in each loading. It can be influenced by variations in amplitude and frequency. Its damage for each loading cycle D_i is:

$$D_i = \frac{1}{N_f} \tag{9}$$

Palmgren-Miner rule [14,15] was used to determine the cumulative fatigue damage, as follows:

$$D = \Sigma\left(\frac{n_i}{N_f}\right) \tag{10}$$

3. Results and Discussion

Analysis from the chemical composition testing results shows that the material for the coil spring consited of 0.64 % carbon (C), 0.16 % silicon (Si), 0.77 % manganese (Mn), 0.76 % chromium (Cr), 0.18 % molybdenum (Mo), 0.15 % vanadium (V), 0.01 % sulfur (S) and 0.003 % phosphor (P). Therefore, it can be concluded that the coil spring was made from the SAE 5160 carbon steel [16], used in the automotive industries. Table 1 presents its mechanical properties.

Table 1. The mechanical propertis of the SAE5160 carbon steel [17].

Properties	Values
Ultimate tensile strength, S_u (MPa)	1,584
Material modulus of elasticy, E (GPa)	207
Yield strength [MPa]	1,487
Fatigue strength coefficient, σ'_f (MPa)	2,063
Fatigue strength exponent, b	-0.08
Fatigue ductility exponent, c	-1.05
Fatigue ductility coefficient, ε'_f	9.56
Cyclic strain-hardening exponent	0.05
Cyclic strength coefficient (MPa)	1,940
Poison ratio	0.27

The stress concentrations are available in several color contours as shown in figure 3. The area with the highest stress concentration is represented by red, orange, yellow, green and blue. The red area has a maximum von Mises stress of 0.997 GPa. With reference to table 1, the maximum stress was low in comparison to the yield strength of the SAE 5160 carbon steel, which was 1.487 GPa. This illustrated that the load did not collapse the component. The surface area of the inner spring was smaller than the outside so that the critical point occurred in the inside. This was identical to other research results [18-21].

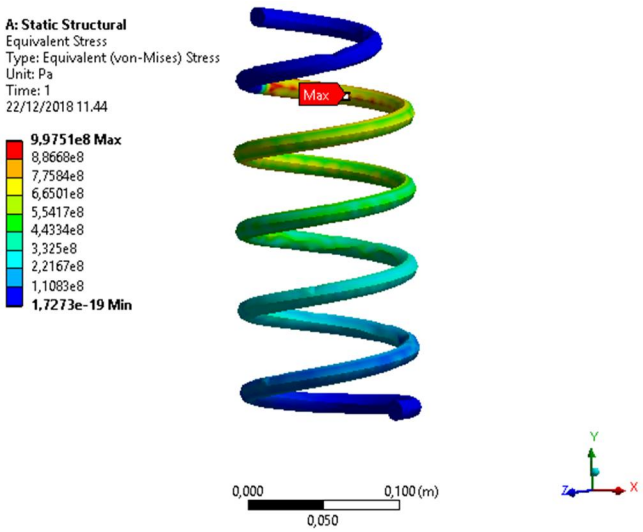

Figure 3. Stress distribitions of the coil spring.

30,000 data gave a total length of 60 seconds as shown in figure 4. All strain signals have non-zero-mean values, which were -684 με and -658 με for the smooth and rough road surfaces, respectively. The negative mean value indicated that the coil spring received a compressive load. The smooth and rough roads provided the SD of 20 με and 22 με, while for the r.m.s., their values were 685 με and 658 με, respectively. Both signals were non-stationary as displayed on the kurtosis above 3 [22,23], which was 4.1 and 5.8.

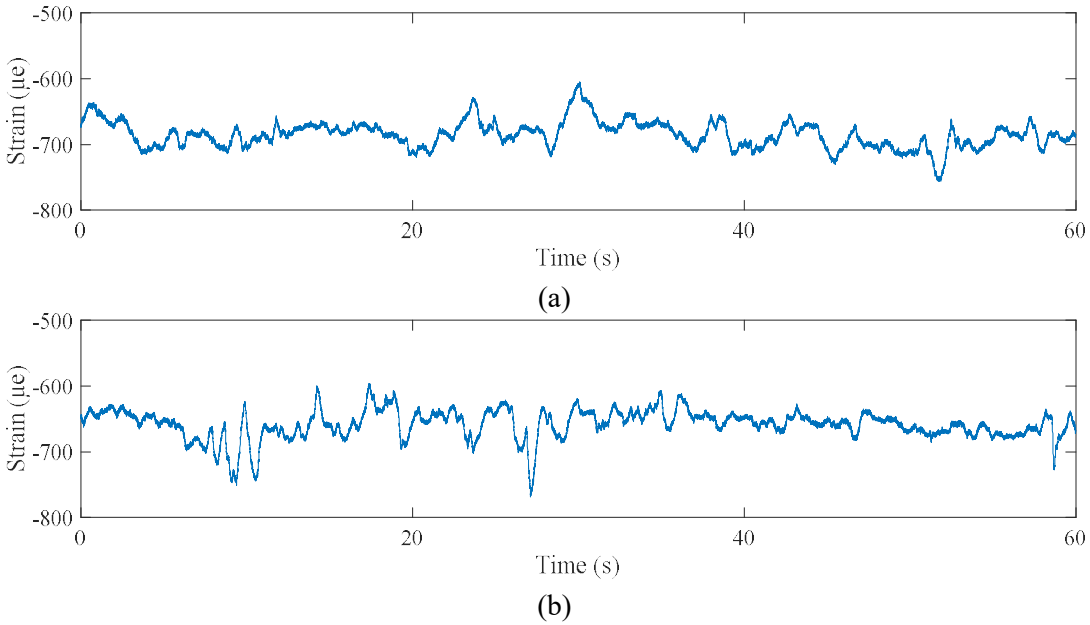

Figure 4. Strain signals: (a) smooth, (b) rough.

Based on the Coffin-Manson model, the fatigue damage for the smooth and rough roads was 2.9E-2 damage per block and 4.9E-2 damage per block, respectively. Using the Morrow model, it was 2.2E-2 damage per block and 4.1E-2 damage per block. For the SWT model, it was 1E-2 damage per block and 2.5E-2 damage per block. A higher damage caused a decrease of the fatigue life in the coil spring. Therefore, the rough road provided a shorter fatigue life, which was 1,284 cycles to failure with a higher vertical load contour, while the smooth road gave 19,060 cycle to failure.

4. Conclusion

This study aims to determine the effect of road surface contours on the fatigue life of a vehicle coil spring. According the results, it can be concluded that just as a vehicle plies a rough road surface, the coil spring received a higher stress contributing to a shorter fatigue life. It also accelerated the useful life of the coil spring by 526 %.

5. Acknowledgements

The authors would like to express their gratitude to Universitas Syiah Kuala for financial support for this research through the grant No. 55/UN11.2/PP/SP3/2019 and 63/UN11.2/PP/PNBP/SP3/2019.

6. References

[1] Jin L Q, Ling M, Yue W 2017 *PLoS ONE* **12**.
[2] Ansari A A, Jain K K 2016 *Global J. Eng. Sci. Res.* **3**.
[3] Kumhar V 2016 *VSRD Int. J. Mechanic. Civil, Automobile Product. Eng.* **6**.
[4] Cruz M L S, Carrillo J, de Almeida S F M 2016 *Latin American J. Solids Struct.* **13** 435-55.
[5] Mahalov M S, Blumenstein V Y 2016 *IOP Conf. Series: Mater. Sci. Eng.* **126**.
[6] Yanxun X, Da T, Mingxi D, Yunze L, Changjun L, Fuzhen X 2018 *Metals* **8**.

[7] Mulia T M, Kadam S J, Kengar V S 2012 *Int. J. Mechanic. Industrial Eng.* **2** 74-7.
[8] Von Mises R 1913 *Mathematisch-Physikalische Klasse 1* 582-92.
[9] Ilic S 2006 *Methodology of Evaluation of In-Service Load Applied to the Output Shafts of Automatic Transmissions* Ph.D. Thesis The University of New South Wales.
[10] Coffin Jr. L F 1954 *Transactions of the ASME* **76** 931-50.
[11] Manson S S 1965 *Experimental Mechanics* **5** 193-226.
[12] Morrow J 1968 *Fatigue Design Handbook* Society of Automotive Engineers.
[13] Smith K N, Watson P, Topper T H 1970 *J. Mater. JMLSA* **5** 767-78.
[14] Palmgren A 1924 *Zeitschrift VDI* **68** 339-41.
[15] Miner M A 1945 *J. Appl. Mechanic.* **67** A159-64.
[16] ASTM A322-91 2001 *Standard Specification for Steel Bars, Alloy, Standard Grades* ASTM International.
[17] nCode 2018 *GlyphWorks* nCode International, Ltd.
[18] Zhu Y, Wang Y, Huang Y 2014 *Case Studies in Engineering Failure Analysis* **2** 169-73.
[19] Putra T E, Abdullah S, Schramm D, Nuawi M Z, Bruckmann T 2015 *Mechanical Systems and Signal Processing* **60-61** 485-97.
[20] Putra T E, Abdullah S, Schramm D, Nuawi M Z, Bruckmann T 2017 *Mechanical Systems and Signal Processing* **90** 1-14.
[21] Putra T E, Abdullah S, Schramm D, Nuawi M Z, Bruckmann T 2017 *Mechanical Systems and Signal Processing* **94** 432-47.
[22] Chen X 2014 *Engineering Structures* **74** 145-56.
[23] Kihm F, Ferguson N S, Antonic J 2015 *Procedia Engineering* **133** 698-713.